

## TECHNICAL REPORT

# Effect of Cell Labeling on the Function of Human Pluripotent Stem Cell-Derived Cardiomyocytes

Seong Woo Choi<sup>1</sup>, Young-Woo Cho<sup>2,3</sup>, Jae Gon Kim<sup>4</sup>, Yong-Jin Kim<sup>5</sup>,  
Eunmi Kim<sup>5</sup>, Hyung-Min Chung<sup>6</sup>, Sun-Woong Kang<sup>7</sup>

<sup>1</sup>*Ischemic/Hypoxic Disease Institute, Seoul National University College of Medicine, Seoul, Korea*

<sup>2</sup>*Department of Pharmacy, Chungbuk National University College of Pharmacy, Cheongju, Korea*

<sup>3</sup>*Division of Drug Evaluation, NDDC, Oseong Medical Innovation Foundation, Cheongju, Korea*

<sup>4</sup>*Research Group for Biomimetic Advanced Technology, Korea Institute of Toxicology, Daejeon, Korea*

<sup>5</sup>*R&D Unit, Amorepacific Corporation, Yongin, Korea*

<sup>6</sup>*Department of Stem Cell Biology, School of Medicine, Konkuk University, Seoul, Korea*

<sup>7</sup>*Department of Human and Environmental Toxicology, University of Science and Technology, Daejeon, Korea*

Cell labeling technologies are required to monitor the fate of transplanted cells in vivo and to select target cells for the observation of certain changes in vitro. Human induced pluripotent stem cell-derived cardiomyocytes (hiPSC-CMs) have been transplanted for the treatment of heart injuries or used in vitro for preclinical cardiac safety assessments. Cardiomyocyte (CM) labeling has been used in these processes to facilitate target cell monitoring. However, the functional effect of the labeling agent on hiPSC-CMs has not been studied. Therefore, we investigated the effects of labeling agents on CM cellular functions. <sup>32</sup>-Diiodoacetylfluorescein perchlorate (DiO), quantum dots (QDs), and a DNA plasmid expressing EGFP using Lipo2K were used to label hiPSC-CMs. We conclude that the hiPSC-CM labeling with DiO and QDs does not induce arrhythmogenic effects but rather improves the mRNA expression of cardiac ion channels and Ca<sup>2+</sup> influx by L-type Ca<sup>2+</sup> channels. Thus, DiO and QD labeling agents may be useful tools to monitor transplanted CMs, and further in vivo influences of the labeling agents should be investigated in the future.

**Keywords:** Stem cells, Cardiomyocytes, Cell labeling, Alternative model, Direct label

Received: November 15, 2019, Revised: March 1, 2020,

Accepted: March 3, 2020, Published online: April 30, 2020

Correspondence to **Sun-Woong Kang**

Department of Human and Environmental Toxicology, University of Science and Technology, 141 Gajeong-ro, Yuseong-gu, Daejeon 34114, Korea

Tel: +82-42-610-8209, Fax: +82-42-610-8157

E-mail: [swkang@kitox.re.kr](mailto:swkang@kitox.re.kr)

Co-Correspondence to **Hyung-Min Chung**

Department of Stem Cell Biology, School of Medicine, Konkuk University, 120 Neungdong-ro, Gwangjin-gu, Seoul 05029, Korea

Tel: +82-2-2049-6028, Fax: +82-2-455-9012

E-mail: [hmchung@kku.ac.kr](mailto:hmchung@kku.ac.kr)

© This is an open-access article distributed under the terms of the Creative Commons Attribution Non-Commercial License (<http://creativecommons.org/licenses/by-nc/4.0/>), which permits unrestricted non-commercial use, distribution, and reproduction in any medium, provided the original work is properly cited.

Copyright © 2020 by the Korean Society for Stem Cell Research

## Introduction

Cell labeling knowledge has significantly increased, resulting in the development of numerous labeling agents, including fluorescent probes, superparamagnetic iron oxide, radiotracers, and genetic modifications (1). Indeed, a wide variety of labeling agents have been used to distinguish target cells from neighboring cells and monitor the functional effects of target cells. Several studies have reported that the labeling mechanism typically involves the adherence and diffusion of a lipophilic cyanine-based dye across the phospholipid cell membrane bilayer. Other modes include transporters, endocytosis, and phagocytosis (2, 3).

The transportation of labeling agents into the cells could change the biological responses of cells, such as metabolism, proliferation, and migration (4-6). Labeling agent-rich regions cause changes in the physical properties of the cell surface and thereby determine cellular characteristics, i.e., the cell surface, repulsion between cells, subsequent migration, and the uptake of ion (7-9). Ideal labeling agents should have high labeling efficiency and not have harmful effects on cellular function. In previous studies, various labeling agents have been used to efficiently label cardiomyocytes (CMs) for in vivo tracking (10-13). However, these studies did not focus on the functional effects on CMs. In particular, the influence of labeling on the physiological functions of human induced pluripotent stem cell-derived cardiomyocytes (hiPSC-CMs) should be verified. hiPSC-CMs are considered a promising option for future applications in various fields (14-16). The electrophysiological dysfunction of hiPSC-CMs can lead to negative application consequences, such as abnormal drug reactions when assessing cardiac toxicity or lethal arrhythmia in heart failure treatment with injected CMs (17-19). In addition, low cell retention and engraftment rates are another safety risk for stem cell-based therapies, so the labeling of CMs is required for long-term monitoring (20-22). Despite the importance of hiPSC-CM function and labeling, no studies have evaluated the effect of labeling agents on hiPSC-CMs.

Therefore, the purpose of this study was to investigate the effects of three different labeling agents on the cellular functions of CMs. Thus, CMs were labeled with 3'-diiodoacetylcarbocyanine perchlorate (DiO), quantum dots (QDs), and plasmid DNA expressing EGFP using Lipo2K. The labeled cells were subsequently characterized at the cellular functional and molecular levels. The results of this study may provide useful tools to expand the potential applications of CM labeling.

## Materials and Methods

### Human iPSC-derived cardiomyocyte culture

hiPSC-derived CMs (iCell<sup>®</sup>) and cell culture medium (iCell Cardiomyocyte Maintenance Medium) were purchased from Cellular Dynamics International (CDI, Madison, WI, USA). Cells were thawed and handled according to the manufacturer's guidelines. The cells were plated at  $2 \times 10^4$  cells/well and maintained at 37°C with 5% CO<sub>2</sub> and 95% humidity. Cells began to beat spontaneously within one or two days of plating. Cell labeling was performed at 7 days after plating.

### Cell labeling and the measurement of labeling efficacy

The CMs were labeled with DiO (Vybrant cell labeling solution, Molecular Probes, Eugene, OR), QD 525 (Thermo Fisher Scientific, Rockford, IL, USA), and pcDNA3-EGFP using Lipofectamine 2000 (Lipo2K; Invitrogen, Carlsbad, CA, USA). For labeling, cells were treated with DiO, 5 μM dye working solution for 10 min. After treatment, the dye working solution was removed, and the cells were washed three times with growth medium. For EGFP labeling using Lipo2K, CMs were transfected with 100 ng of pcDNA3-EGFP using Lipo2K according to the manufacturer's instructions. Branched polyethyleneimine (BPEI; 25 kDa) was prepared at an N/P ratio of 20/1. The cells were seeded on well plates, the culture medium was replaced with transfection medium containing Lipo2K complexes, and the plate was incubated for 6 h at 37°C. Then, the transfection medium was replaced with fresh growth medium, and the cells were maintained for 2 days. After incubation, the cells were washed twice with DPBS (pH 7.4). For QD labeling, cells were incubated in medium containing 1 μM QD 525 for 6 h at 37°C, and cells were washed three times with DPBS. Then, the samples were analyzed using laser-scanning confocal microscopy (LSM 710, Carl Zeiss, Thornwood, NY, USA).

### Cell viability assay

To measure cell viability after labeling, CMs were seeded on 96-well plates ( $5 \times 10^3$  cells/well) and incubated for 1 day. After labeling, cell counting kit-8 solution (10 μl; Dojindo Molecular Technologies Inc., Kumamoto, Japan) was added to each well. After further incubation for 2 h at 37°C, the absorbance of each well was measured at 450 nm using a microplate reader (iMmark, Microplate Absorbance Reader, Bio-Rad, CA, USA).

### Real-time quantitative PCR

Total RNA was extracted from heart tissue with TRIzol (Invitrogen, Carlsbad, CA, USA) and reverse-transcribed using a complementary DNA reverse transcription kit (Invitrogen, Carlsbad, CA, USA). Reactions were performed in a real-time PCR thermocycler (Applied Biosystem, Foster City, CA, USA) using SYBR green as the fluorescence dye. The mRNA expression of the target genes was normalized to that of the control glyceraldehyde-3-phosphate dehydrogenase (GAPDH) using the comparative threshold cycle method. Quantitative PCR was performed using SYBR Green PCR Master Mix (2×; Promega, Madison, WI, USA) and 0.2 μM of the following gene-specific primers: forward primer, 5'-TTCTATTACCTCGGGGCAC-3' and reverse primer, 5'-TGCCATAGAGATCTGGCAGC-

3' for SCN5A; forward primer, 5'-ATACCAGCCGCTCTC CAGTT-3' and reverse primer, 5'-ACTGCCCATTA ACTT GGCCT-3' for CACNA1c; forward primer, 5'-ACTACAT CATCCGGAAGGC-3' and reverse primer, 5'-CAGCAG GCAGATCTCTCCAA-3' for HCNA4; forward primer, 5'-TCCTCTGTGTGGGTTCCAAA-3' and reverse primer, 5'-CCGACTCATTCATGCATC-3' for KCNQ1; forward primer, 5'-CATCTACTGCAACGACGGCT-3' and reverse primer, 5'-GACAGCCCCATCTCATTCT-3' for KCNH2; forward primer, 5'-CCCAATTGCTGTTTTTCATGG-3' and reverse primer, 5'-GTCTCTCATGGCAATCACGG-3' for KCNJ2; and forward primer, 5'-CCCATGTTTCGTCATGG GTGT-3' and reverse primer, 5'-TGGTCATGAGTCCTTC CACGATA-3' for GAPDH. The cycle conditions were as follows: primary denaturation at 95°C for 3 min, 40 cycles of 6 s at 95°C, 60 s at 60°C, and 60 s at 72°C, followed by fluorescence measurement. The expression of target genes was normalized using GAPDH as a reference gene.

### Electrophysiological recording

Conventional whole-cell patch-clamp was performed to record the action potential (AP) and currents. The signals were amplified and digitized with an Axopatch 200B amplifier (Axon Instruments, Foster, CA, USA) and a Digidata 1440B AD-DA converter (Axon Instruments). pClamp 10.1 (Axon Instruments) and Origin 8.0 (Microcal, Northampton, MA, USA) were used for the analysis of AP parameters and current amplitudes. Microglass pipettes (World Precision Instruments, Sarasota, FL, USA) were pulled to the resistance of 2~3 M $\Omega$  with a PP-830 puller (Narishige, Tokyo, Japan). The extracellular buffer solution for recording AP activity contained (in mM) 145 NaCl, 5.4 KCl, 10 HEPES, 1 MgCl<sub>2</sub>, 1.8 CaCl<sub>2</sub>, and 5 glucose adjusted to pH 7.4 with NaOH. The intracellular solution contained (in mM) 120 K-aspartate, 20 KCl, 5 NaCl, 2 CaCl<sub>2</sub>, 5 EGTA, 10 HEPES, and 5 MgATP adjusted to pH 7.25 with KOH. The extracellular buffer solution for I<sub>Ca,L</sub> contained (in mM) 145 CsCl, 10 HEPES, 1 MgCl<sub>2</sub>, 1.8 CaCl<sub>2</sub> and 5 glucose adjusted to pH 7.4 with CsOH. The intracellular solution for I<sub>Ca,L</sub> contained (in mM) 106 CsCl, 5 NaCl, 20 TEA-Cl, 10 HEPES, 5 MgATP, and 1 EGTA adjusted to pH 7.25 with CsOH. I<sub>Ca,L</sub> was recorded using a stepwise protocol with a holding potential of -50 mV and depolarization from -40 to 40 mV in 10-mV increments. The extracellular buffer solution for I<sub>Nav</sub> contained (in mM) 135 CsCl, 20 NaCl, 10 HEPES, 1 MgCl<sub>2</sub>, 1.8 CaCl<sub>2</sub>, 0.1 CdCl<sub>2</sub>, and 5 glucose adjusted to pH 7.4 with CsOH. The intracellular solution for I<sub>Nav</sub> contained (in mM) 135 CsCl, 5 NaCl, 10 HEPES, 5 MgATP, and 10 EGTA adjusted to pH 7.25 with CsOH. To assess

the peak amplitude of the I<sub>Nav</sub> density, cells were held at -100 mV and depolarized to various test step voltages (from -80 to 40 mV in 10 mV steps).

### Statistical analysis

Quantitative data were expressed as the mean  $\pm$  standard deviation. Statistical comparisons were carried out using ANOVA tests (SPSS Inc., Chicago, IL, USA). A probability level of less than 0.05 was considered statistically significant.

### Results

The hiPSC-CMs were thawed, plated in plating medium, maintained in maintenance medium, and begin to beat spontaneously within 2 days of plating. After the cells were labeled with three different agents (DiO, QDs, and EGFP using Lipo2K), the fluorescence labeling efficiency was analyzed on days 1, 7, and 14. One day after culture, 97.5 and 99.4% of the inoculated hiPSC-CMs were labeled with DiO and QDs, whereas only 33.7% expressed GFP (Fig. 1). The number of hiPSC-CMs labeled with DiO and QDs was maintained over the culture time. The labeling

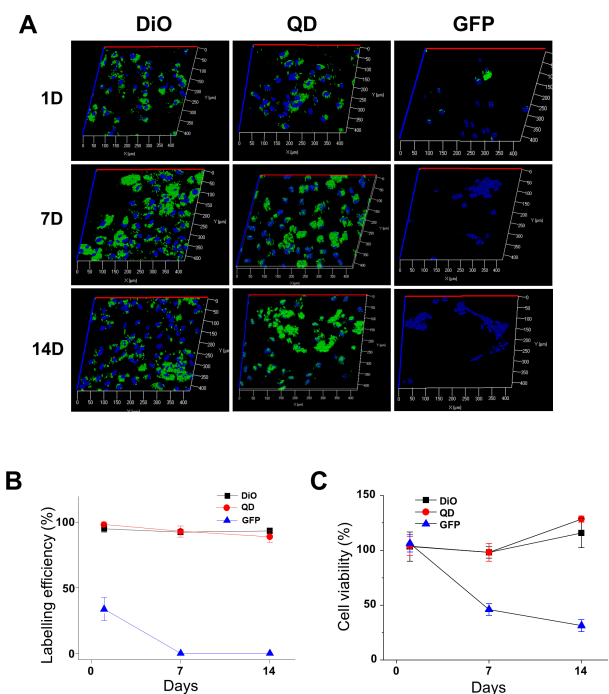


**Fig. 1.** Analysis of the labeling efficiency and cell viability of three labeling agents: DiO, QD, and GFP using Lipo2K. (A, B) The efficiency of the three agents was analyzed by green fluorescence at 1 day, 7 days, and 14 days after labeling. (C) Cell viability after labeling was analyzed on the same days.

efficacy of both DiO and the QDs remained similar over 14 days. In contrast, the number of GFP-labeled cells and viability decreased significantly over the culture time. Cytotoxicity of Lipo2K has been reported for many cell lines, but EGFP-labeling using Lipo2K showed much lower viability in hiPSC-CMs compared to COS (CV-1 in Origin, and carrying SV40 genetic material) and other immortal cell lines (23, 24). This result suggests that Lipo2K, a liposomal transfection reagent with exogenous DNA is not a suitable labeling method for hiPSC-CMs.

Next, we examined whether DiO and QD labeling influences the mRNA expression of the essential cardiac ion channels ( $K^+$  channel; KCNA4, KCNQ1, KCNH2, and KCNJ2, L-type  $Ca^{2+}$  channel; CACNA1c, voltage-dependent  $Na^+$  channel; SCN5A, and hyperpolarization-activated cyclic nucleotide-gated channel; HCN4) of hiPSC-CMs (Fig. 2). There was no significant difference in the mRNA

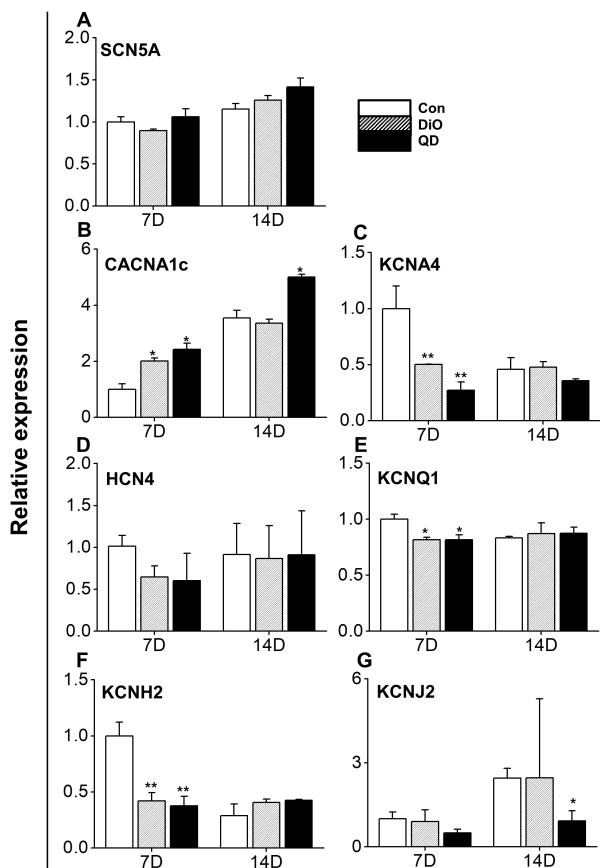


**Fig. 2.** The effects of DiO and QD labeling on mRNA expression of cardiac ion channels. (A~G) Changes in the expression of SCN5A, CACNA1c, KCNA4, HCN4, KCNQ1, KCNH2, and KCNJ2 in hiPSC-CMs were observed at 7 and 14 days after DiO and QD labeling. All the data were analyzed using paired *t*-tests, where  $p < 0.05$  (\*) and  $p < 0.01$  (\*\*) were considered statistically significant.

expression between the control cells and the labeled cells over the 14 days after labeling. When the mRNA expression of SCN5A, CACNA1c, and KCNJ2 in the control cells increased, that of the labeled cells also increased. At 7 days after labeling, the mRNA expression of CACNA1c, KCNH2, KCNA4, and KCNQ1 in the labeled group was significantly different from that in the control group. Over time, the difference in KCNH2, KCNA4, and KCNQ1 mRNA expression was reduced. Overall, there was no dif-

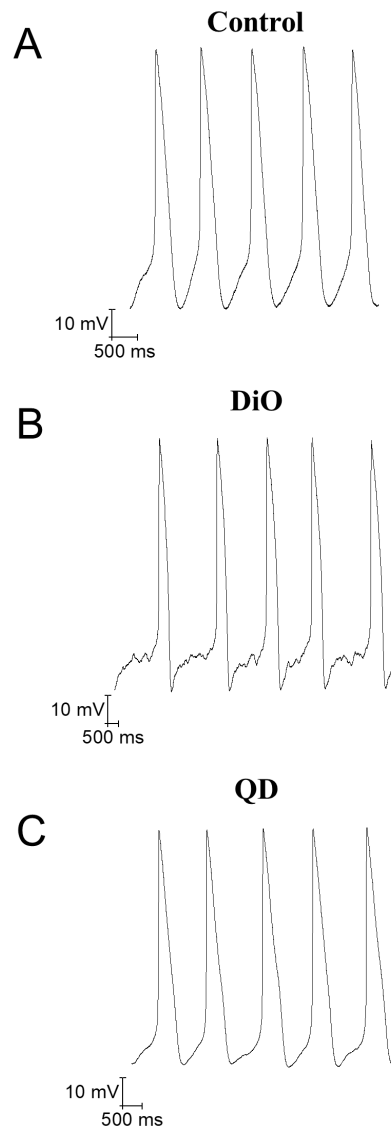


**Fig. 3.** The AP activity of hiPSC-CMs was recorded after 7 days of DiO and QD labeling, and its characteristics were analyzed. (A~C) Spontaneous AP activity of control, DiO, and QD-labeled hiPSC-CMs. The action potentials were analyzed as the APA, MDP,  $V_{max}$ , and  $APD_{90}$  (Table 1). All the data were analyzed using paired *t*-tests, where a  $p < 0.05$  was considered statistically significant.

**Table 1.** Analysis of action potential properties in control, DiO, QD-labeled hiPSC-CMs

Labeling probe	APA (mV)	MDP (mV)	Vmax (V/s)	APD90 (mV)
Control (n=5)	86.3±4.8	-59.2±4.1	8.1±2.3	447.3±37.8
DiO (n=5)	91.4±5.5	-52.0±5.1	13.1±6.9	473.5±49.0
QDs (n=5)	84.8±1.9	-51.0±1.9	7.76±1.4	457.9±67.3

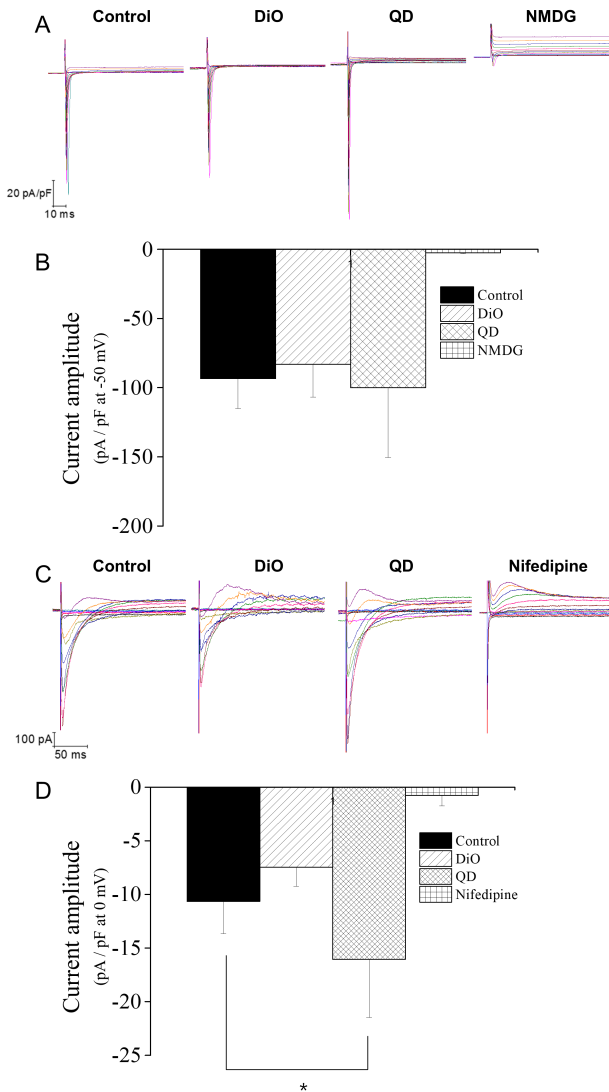


**Fig. 4.** Effect of DiO and QD labeling on the voltage-dependent  $Na^+$  current ( $I_{NaV}$ ) and L-type  $Ca^{2+}$  current ( $I_{Ca,L}$ ) in hiPSC-CMs. (A, B) Peak amplitudes of  $I_{NaV}$  were analyzed after replacing  $Na^+$  in the extracellular solution with  $NMDG^+$ . The peak inward current densities recorded in DiO- and QD-labeled CMs compared to unlabeled control CMs at  $-50$  mV. (C, D) Peak amplitudes of  $I_{Ca,L}$  were analyzed after the application of a selective inhibitor, nifedipine ( $1 \mu M$ ). A significant increase in  $I_{Ca,L}$  was observed in QD-labeled CMs compared to control CMs. All the data were analyzed using paired *t*-tests, where  $*p < 0.05$  was considered statistically significant.

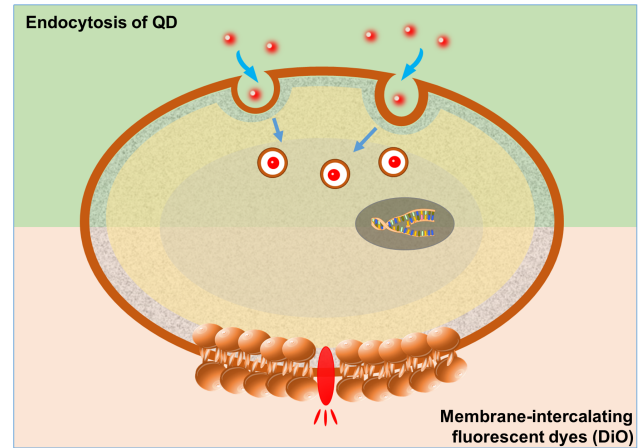


**Fig. 5.** Illustration of labeling mechanism for DiO and QD.

ference in the mRNA expression between the DiO and QD labeled groups.

Finally, we validated whether the action of DiO and QDs affect the CM electrophysiological profile. The effects of DiO and QDs on the APs and ion channel currents were evaluated in the hiPSC-CMs at day 7 after labeling because the change in ion channel gene expression was the greatest at day 7 after labeling. APs from non-treated control or DiO- and QD-labeled hiPSC-CMs were recorded and analyzed (Fig. 3). DiO and QD labeling agents did not affect the AP amplitude (APA), maximum diastolic potential (MDP), maximum upstroke velocity ( $V_{max}$ ), and action potential duration 90% ( $APD_{90}$ ). The parameters are presented in Table 1.

The voltage-dependent  $Na^+$  current ( $I_{NaV}$ ) and L-type  $Ca^{2+}$  current ( $I_{Ca,L}$ ) in hiPSC-CMs were recorded using the voltage-clamp patch-clamp method. The subtracted currents were obtained by substitution of extracellular  $Na^+$  with  $NMDG^+$  and by applying nifedipine, a specific inhibitor of  $I_{Ca,L}$ . The peak amplitude of  $I_{NaV}$  at  $-50$  mV was analyzed between control and DiO- or QD-labeled CMs. The amplitude of  $I_{NaV}$  in DiO- and QD-labeled cells was not different from that in control cells (Fig. 4A and 4B). The peak amplitude of  $I_{Ca,L}$  at  $0$  mV was analyzed. Compared to the control CMs, QD-labeled CMs had an

increased amplitude of  $I_{Ca,L}$ , but the DiO-labeled CM amplitude showed no conversion (Fig. 4C and 4D).

## Discussion

Many hurdles remain to the widespread acceptance of labeling for cell tracking and labeling for stem cell-derived cardiomyocytes because the functional changes of labeling agents in cells are not fully understood. Although these materials have biocompatibility in the cells, many previous studies have shown that the carbocyanine dyes with highly lipophilic nature and nano-materials such as QD specifically led to changes in bio-physiological function, cellular signaling pathways and interference with cell-cell communication (4-6, 25, 26). Indeed, carbocyanine dyes showed at high concentrations in cancer cell lines (6). The QD negatively affected cell growth and migration functions (25, 26). Thus, if these labeling agents are to be used for stem cell-derived cardiomyocytes, its effects on physiological properties, biochemical properties of modified cells, and cellular function should be clearly defined.

This study is the first to evaluate the functional effect of labeling agents on hiPSC-CMs. hiPSC-CMs were labeled with DiO and QDs with high efficiency and without cytotoxic effects. However, labeling with EGFP using Lipo2K, a transfection reagent, significantly reduced cell viability. Labeling with DiO and QDs did not have negative electrophysiological influences, such as arrhythmogenic effects, including the early and delayed after-depolarizations of AP or prolongation of AP in hiPSC-CMs. Rather, QD labeling increased  $Ca^{2+}$  influx through the enhancement of  $I_{Ca,L}$ .

Direct labeling is more consistent and effective than indirect labeling in hiPSC-CMs. We selected DiO and QDs for the direct labeling method because DiO and QD labeling have proven to be sufficient for various cell labeling applications in vitro. Cells labeled with both types of labels showed higher fluorescence intensities than untreated cells (Fig. 1). Generally, one of the disadvantages of direct labeling methods is that the labeling agent becomes diluted when cells proliferate, resulting in decreased fluorescence intensity of the labeling agent per cell (27-30). This factor usually limits the time available for the observation of directly labeled cells. However, hiPSC-CMs exhibit very low levels of proliferation (31, 32). Thus, the dilution of the labeling agent in the cell by cell division does not occur. Indeed, the intensity of hiPSC-CMs labeled with DiO and QDs was similar on the first and the 14<sup>th</sup> day after labeling (Fig. 1). These results indicate that direct labeling methods are suitable for hiPSC-CMs with

low proliferative activity. The labeling efficacy of the indirect system was also tested with genetic modification using EGFP gene transfection by Lipo2K. It was difficult to transfect the hiPSC-CMs using a nonviral gene transfer delivery system because of the low transfection rates and cell toxicity.

hiPSC-CMs possess similar contractibility, synchronicity, and electrochemical properties as cardiac tissue (33, 34). Therefore, hiPSC-CMs are used for cellular cardiomyoplasty to regenerate the myocardium (35, 36). Indeed, recent studies reported that CMs from pluripotent stem cells were successfully transplanted and repaired the myocardium when injected into the damaged heart of immunosuppressed animals (17, 37-40). In addition, hiPSC-CMs have been developed to replace animal testing for cardiac safety assays (41, 42). For these developments, the functions of hiPSC-CMs, including the repolarization or depolarization of cardiac ion channels and calcium flux, should be maintained. Therefore, the ideal labeling method of hiPSC-CMs should be noncytotoxic and not have harmful effects on other cellular functions. Our results demonstrate the electrophysiological safety of DiO and QD labeling in hiPSC-CMs. Both labeling agents did not significantly change the AP.

Functional immaturity is a well-known property of hiPSC-CMs. According to previous reports, hiPSC-CMs have an immature  $Ca^{2+}$  handling ability and fewer contractile proteins than mature CMs (43, 44). In mature CMs, the excitation-contraction (EC) coupling is mediated mainly by calcium-induced calcium release, whereas it is predominantly due to the trans-sarcolemmal influx of  $Ca^{2+}$  in hiPSC-CMs (43). Our results demonstrate that QD labeling enhances  $Ca^{2+}$  influx (Fig. 4C) and mRNA expression of CACNA1c (Fig. 2B). DiO and QD labelings promoted mRNA expression of  $Ca^{2+}$  and  $K^+$  ion channels. In both control and labeled groups, mRNA expression of  $Ca^{2+}$  and  $K^+$  ion channels increased over 14 days. Interestingly, mRNA expression of  $Ca^{2+}$  and  $K^+$  ion channels, which was expressed in 14 days in control group, was expressed in 7 days in DiO and QD labeled groups (Fig. 2B, 2C, 2E, and 2F). Increased  $Ca^{2+}$  influx and enhanced ion channel expression may improve the  $Ca^{2+}$  handling and electrophysiological properties of immature EC coupling in hiPSC-CMs, although we do not present direct evidence of  $Ca^{2+}$  and CM contraction.

In conclusion, we demonstrated that DiO and QD labeling of hiPSC-CMs is stable, long-lasting, non-toxic, and may allow safe and long-term cell tracking to monitor CM-based therapies. Since this study was conducted in vitro, it is necessary to confirm the safety and efficacy of

the labeled CMs in vivo in further studies.

### Acknowledgments

This work supported by grants (NRF-2019M3A9H1103331 and NRF-2017M3A9C7065685) from National Research Foundation funded by the Ministry of Science and ICT, Korea.

### Potential Conflict of Interest

The authors have no conflicting financial interest.

### References

- Zhang SJ, Wu JC. Comparison of imaging techniques for tracking cardiac stem cell therapy. *J Nucl Med* 2007;48:1916-1919
- Fernando LP, Kandel PK, Yu J, McNeill J, Ackroyd PC, Christensen KA. Mechanism of cellular uptake of highly fluorescent conjugated polymer nanoparticles. *Biomacromolecules* 2010;11:2675-2682
- Lee SY, Lee S, Lee J, Yhee JY, Yoon HI, Park SJ, Koo H, Moon SH, Lee H, Cho YW, Kang SW, Lee SY, Kim K. Non-invasive stem cell tracking in hindlimb ischemia animal model using bio-orthogonal copper-free click chemistry. *Biochem Biophys Res Commun* 2016;479:779-786
- Han SS, Lee DE, Shim HE, Lee S, Jung T, Oh JH, Lee HA, Moon SH, Jeon J, Yoon S, Kim K, Kang SW. Physiological effects of Ac4ManNAz and optimization of metabolic labeling for cell tracking. *Theranostics* 2017;7:1164-1176
- Han SS, Shim HE, Park SJ, Kim BC, Lee DE, Chung HM, Moon SH, Kang SW. Safety and optimization of metabolic labeling of endothelial progenitor cells for tracking. *Sci Rep* 2018;8:13212
- Kang SW, Lee S, Na JH, Yoon HI, Lee DE, Koo H, Cho YW, Kim SH, Jeong SY, Kwon IC, Choi K, Kim K. Cell labeling and tracking method without distorted signals by phagocytosis of macrophages. *Theranostics* 2014;4:420-431
- Zhang S, Gao H, Bao G. Physical principles of nanoparticle cellular endocytosis. *ACS Nano* 2015;9:8655-8671
- Karabanovas V, Zitkus Z, Kuciauskas D, Rotomskis R, Valius M. Surface properties of quantum dots define their cellular endocytic routes, mitogenic stimulation and suppression of cell migration. *J Biomed Nanotechnol* 2014;10:775-786
- Ni SD, Yin YW, Li XL, Ding HM, Ma YQ. Controlling the interaction of nanoparticles with cell membranes by the polymeric tether. *Langmuir* 2019;35:12851-12857
- Templin C, Zweigerdt R, Schwanke K, Olmer R, Ghadri JR, Emmert MY, Müller E, Küest SM, Cohrs S, Schibli R, Kronen P, Hilbe M, Reinisch A, Strunk D, Haverich A, Hoerstrup S, Lüscher TF, Kaufmann PA, Landmesser U, Martin U. Transplantation and tracking of human-induced pluripotent stem cells in a pig model of myocardial infarction: assessment of cell survival, engraftment, and distribution by hybrid single photon emission computed tomography/computed tomography of sodium iodide symporter transgene expression. *Circulation* 2012;126:430-439
- Berninger MT, Mohajerani P, Wildgruber M, Beziere N, Kimm MA, Ma X, Haller B, Fleming MJ, Vogt S, Anton M, Imhoff AB, Ntziachristos V, Meier R, Henning TD. Detection of intramyocardially injected DiR-labeled mesenchymal stem cells by optical and optoacoustic tomography. *Photoacoustics* 2017;6:37-47
- Pei Z, Zeng J, Song Y, Gao Y, Wu R, Chen Y, Li F, Li W, Zhou H, Yang Y. In vivo imaging to monitor differentiation and therapeutic effects of transplanted mesenchymal stem cells in myocardial infarction. *Sci Rep* 2017;7:6296
- Silva AK, Wilhelm C, Kolosnjaj-Tabi J, Luciani N, Gazeau F. Cellular transfer of magnetic nanoparticles via cell microvesicles: impact on cell tracking by magnetic resonance imaging. *Pharm Res* 2012;29:1392-1403
- Zhao Y, Korolj A, Feric N, Radisic M. Human pluripotent stem cell-derived cardiomyocyte based models for cardiotoxicity and drug discovery. *Expert Opin Drug Saf* 2016;15:1455-1458
- Ban K, Bae S, Yoon YS. Current strategies and challenges for purification of cardiomyocytes derived from human pluripotent stem cells. *Theranostics* 2017;7:2067-2077
- Denning C, Borgdorff V, Crutchley J, Firth KS, George V, Kalra S, Kondrashov A, Hoang MD, Mosqueira D, Patel A, Prodanov L, Rajamohan D, Skarnes WC, Smith JG, Young LE. Cardiomyocytes from human pluripotent stem cells: from laboratory curiosity to industrial biomedical platform. *Biochim Biophys Acta* 2016;1863(7 Pt B):1728-1748
- Chong JJ, Yang X, Don CW, Minami E, Liu YW, Weyers JJ, Mahoney WM, Van Biber B, Cook SM, Palpant NJ, Gantz JA, Fugate JA, Muskheli V, Gough GM, Vogel KW, Astley CA, Hotchkiss CE, Baldessari A, Pabon L, Reinecke H, Gill EA, Nelson V, Kiem HP, Laflamme MA, Murry CE. Human embryonic-stem-cell-derived cardiomyocytes regenerate non-human primate hearts. *Nature* 2014;510:273-277
- Goineau S, Castagné V. Electrophysiological characteristics and pharmacological sensitivity of two lines of human induced pluripotent stem cell derived cardiomyocytes coming from two different suppliers. *J Pharmacol Toxicol Methods* 2018;90:58-66
- Lei CL, Wang K, Clerx M, Johnstone RH, Hortigon-Vinagre MP, Zamora V, Allan A, Smith GL, Gavaghan DJ, Mirams GR, Polonchuk L. Tailoring mathematical models to stem-cell derived cardiomyocyte lines can improve predictions of drug-induced changes to their electrophysiology. *Front Physiol* 2017;8:986
- Müller-Ehmsen J, Krausgrill B, Burst V, Schenk K, Neisen UC, Fries JW, Fleischmann BK, Hescheler J, Schwinger RH. Effective engraftment but poor mid-term persistence of mononuclear and mesenchymal bone marrow cells in acute and chronic rat myocardial infarction. *J Mol Cell Cardiol* 2006;41:876-884

21. Teng CJ, Luo J, Chiu RC, Shum-Tim D. Massive mechanical loss of microspheres with direct intramyocardial injection in the beating heart: implications for cellular cardiomyoplasty. *J Thorac Cardiovasc Surg* 2006;132:628-632
22. Laflamme MA, Chen KY, Naumova AV, Muskheli V, Fugate JA, Dupras SK, Reinecke H, Xu C, Hassanipour M, Police S, O'Sullivan C, Collins L, Chen Y, Minami E, Gill EA, Ueno S, Yuan C, Gold J, Murry CE. Cardiomyocytes derived from human embryonic stem cells in pro-survival factors enhance function of infarcted rat hearts. *Nat Biotechnol* 2007;25:1015-1024
23. Obata Y, Suzuki D, Takeoka S. Evaluation of cationic assemblies constructed with amino acid based lipids for plasmid DNA delivery. *Bioconjug Chem* 2008;19:1055-1063
24. Arbab AS, Yocum GT, Wilson LB, Parwana A, Jordan EK, Kalish H, Frank JA. Comparison of transfection agents in forming complexes with ferumoxides, cell labeling efficiency, and cellular viability. *Mol Imaging* 2004;3:24-32
25. Diana V, Bossolasco P, Moscatelli D, Silani V, Cova L. Dose dependent side effect of superparamagnetic iron oxide nanoparticle labeling on cell motility in two fetal stem cell populations. *PLoS One* 2013;8:e78435
26. Hardman R. A toxicologic review of quantum dots: toxicity depends on physicochemical and environmental factors. *Environ Health Perspect* 2006;114:165-172
27. Brennan M, Parish CR. Intracellular fluorescent labelling of cells for analysis of lymphocyte migration. *J Immunol Methods* 1984;74:31-38
28. Boutonnat J, Muirhead KA, Barbier M, Mousseau M, Ronot X, Seigneurin D. PKH26 probe in the study of the proliferation of chemoresistant leukemic sublines. *Anticancer Res* 1998;18:4243-4251
29. Parish CR. Fluorescent dyes for lymphocyte migration and proliferation studies. *Immunol Cell Biol* 1999;77:499-508
30. Zhang X, Kiechle FL. Hoechst 33342-induced apoptosis is associated with intracellular accumulation of E2F-1 protein in BC3H-1 myocytes and HL-60 cells. *Arch Pathol Lab Med* 2001;125:99-104
31. Robertson C, Tran DD, George SC. Concise review: maturation phases of human pluripotent stem cell-derived cardiomyocytes. *Stem Cells* 2013;31:829-837
32. Titmarsh DM, Glass NR, Mills RJ, Hidalgo A, Wolvetang EJ, Porrello ER, Hudson JE, Cooper-White JJ. Induction of human iPSC-derived cardiomyocyte proliferation revealed by combinatorial screening in high density microbioreactor arrays. *Sci Rep* 2016;6:24637
33. Giacomelli E, Bellin M, Sala L, van Meer BJ, Tertoolen LG, Orlova VV, Mummery CL. Three-dimensional cardiac microtissues composed of cardiomyocytes and endothelial cells co-differentiated from human pluripotent stem cells. *Development* 2017;144:1008-1017
34. Jackman C, Li H, Bursac N. Long-term contractile activity and thyroid hormone supplementation produce engineered rat myocardium with adult-like structure and function. *Acta Biomater* 2018;78:98-110
35. Moon SH, Kang SW, Park SJ, Bae D, Kim SJ, Lee HA, Kim KS, Hong KS, Kim JS, Do JT, Byun KH, Chung HM. The use of aggregates of purified cardiomyocytes derived from human ESCs for functional engraftment after myocardial infarction. *Biomaterials* 2013;34:4013-4026
36. Park SJ, Kim RY, Park BW, Lee S, Choi SW, Park JH, Choi JJ, Kim SW, Jang J, Cho DW, Chung HM, Moon SH, Ban K, Park HJ. Dual stem cell therapy synergistically improves cardiac function and vascular regeneration following myocardial infarction. *Nat Commun* 2019;10:3123
37. Riegler J, Tiburcy M, Ebert A, Tzatzalos E, Raaz U, Abilez OJ, Shen Q, Kooreman NG, Neofytou E, Chen VC, Wang M, Meyer T, Tsao PS, Connolly AJ, Couture LA, Gold JD, Zimmermann WH, Wu JC. Human engineered heart muscles engraft and survive long term in a rodent myocardial infarction model. *Circ Res* 2015;117:720-730
38. Shiba Y, Fernandes S, Zhu WZ, Filice D, Muskheli V, Kim J, Palpant NJ, Gantz J, Moyes KW, Reinecke H, Van Biber B, Dardas T, Mignone JL, Izawa A, Hanna R, Viswanathan M, Gold JD, Kotlikoff MI, Sarvazyan N, Kay MW, Murry CE, Laflamme MA. Human ES-cell-derived cardiomyocytes electrically couple and suppress arrhythmias in injured hearts. *Nature* 2012;489:322-325
39. Shiba Y, Gomibuchi T, Seto T, Wada Y, Ichimura H, Tanaka Y, Ogasawara T, Okada K, Shiba N, Sakamoto K, Ido D, Shiina T, Ohkura M, Nakai J, Uno N, Kazuki Y, Oshimura M, Minami I, Ikeda U. Allogeneic transplantation of iPSC cell-derived cardiomyocytes regenerates primate hearts. *Nature* 2016;538:388-391
40. Weinberger F, Breckwoldt K, Pecha S, Kelly A, Geertz B, Starbatty J, Yorgan T, Cheng KH, Lessmann K, Stolen T, Scherrer-Crosbie M, Smith G, Reichenspurner H, Hansen A, Eschenhagen T. Cardiac repair in guinea pigs with human engineered heart tissue from induced pluripotent stem cells. *Sci Transl Med* 2016;8:363ra148
41. Guo L, Abrams RM, Babiarez JE, Cohen JD, Kameoka S, Sanders MJ, Chiao E, Kolaja KL. Estimating the risk of drug-induced proarrhythmia using human induced pluripotent stem cell-derived cardiomyocytes. *Toxicol Sci* 2011;123:281-289
42. Harris K, Aylott M, Cui Y, Louttit JB, McMahon NC, Sridhar A. Comparison of electrophysiological data from human-induced pluripotent stem cell-derived cardiomyocytes to functional preclinical safety assays. *Toxicol Sci* 2013;134:412-426
43. Keung W, Boheler KR, Li RA. Developmental cues for the maturation of metabolic, electrophysiological and calcium handling properties of human pluripotent stem cell-derived cardiomyocytes. *Stem Cell Res Ther* 2014;5:17
44. Tan SH, Ye L. Maturation of pluripotent stem cell-derived cardiomyocytes: a critical step for drug development and cell therapy. *J Cardiovasc Transl Res* 2018;11:375-392